# Five-level k·p model for the conduction and valence bands of GaAs and InP

P. Pfeffer and W. Zawadzki
*Institute of Physics, Polish Academy of Sciences, 02-668 Warsaw, Poland*
(Received 20 September 1995)

The band structure of medium-gap semiconductors GaAs and InP is described theoretically using a five-level **k·p** model and including far-level contributions as well as polaron effects. A corresponding theory is also developed to describe orbital and spin properties of charge carriers in both materials in the presence of an external magnetic field of arbitrary orientation. Field dependence of $g$ factors, the spin doublet splittings of the cyclotron resonance, bands' anisotropies, and the energy dependences of the cyclotron masses are described and compared with existing experimental data all the way to the megagauss range of magnetic fields. A good theoretical fit to all the experiments is achieved, which is used to determine the band parameters for GaAs and InP. Values of the polar constants for both materials are discussed. The determined band parameters are employed to calculate the hole masses, which turn out to be in agreement with those found by other authors. It is concluded that the proposed description is adequate for both the conduction and valence bands of GaAs and InP, although there remains a certain ambiguity between the band-structure effects (related to the far-level contributions) and the polaron effects.

## I. INTRODUCTION

GaAs and InP are medium-gap semiconductors of great technological importance. For this reason they have been, in recent years, the subject of numerous experiments, dealing with their bulk properties as well as with the systems of reduced dimensionality. In order to interpret correctly these experiments, one needs to know in detail the band structure of the materials in question. A three-level **k·p** description, successfully used for narrow-gap semiconductors [Kane (Ref. 1), Pidgeon and Brown (Ref. 2)], is not adequate for the medium-gap case, which has been convincingly demonstrated with the use of cyclotron resonance investigations [Zawadzki, Pfeffer, and Sigg (Ref. 3)]. The reason is that in medium-gap semiconductors, the fundamental gap $E_0$ between the $\Gamma_6^c$ and $\Gamma_8^v$ levels is about 1.5 eV, i.e., it is not much smaller than the gap $E_1$ between the $\Gamma_6^c$ level and the upper $\Gamma_7^c$ conduction level (which is about 3 eV).

There have been few attempts to go beyond the three-level model. The published theoretical work can be characterized by two approaches. The first follows the method of Ogg,[4] who used the band decoupling scheme of Luttinger and Kohn[5] to higher orders of the **k·p** perturbation. This way one obtains an effective one-band Hamiltonian, which accounts for band's nonparabolicity (up to $k^4$ terms), nonsphericity, and spin splitting. This method has been pursued by Rossler and co-workers[6,7] for problems without and with magnetic field. It has been demonstrated that the scheme is useful for the description of anisotropic cyclotron resonance data.[8] This formalism, however, has a fundamental shortcoming. It treats the conduction band alone, a description of other bands would require separate developments in powers of **k·p** perturbation, involving separate symmetry considerations, other band parameters, wave functions, etc.

An alternative approach generalizes the work of Kane and of Pidgeon and Brown [cf. also Grisar *et al.* (Ref. 9) and Weiler, Aggarwal, and Lax (Ref. 10)] by going from the three-level model to the five-level model (5LM), which includes exactly the $\Gamma_7^v$, $\Gamma_8^v$, $\Gamma_6^c$, $\Gamma_7^c$, $\Gamma_8^c$ levels in the **k·p** description. This approach has been used by Mycielski *et al.*,[11] Rossler,[12] Cardona, Christensen, and Fasol,[13] and Pikus.[14] The most complete treatment along these lines has been worked out by Pfeffer and Zawadzki,[15] who described in detail various properties of conduction electrons in GaAs and determined important band parameters. A similar work has been carried out for InP by Hopkins *et al.*[16] These papers are concerned with the description of conduction bands, for which it is enough to account for far-level contributions to the **k·p** treatment by adding small constants to the effective mass and the spin $g^*$ factor (cf. Hermann and Weisbuch, Ref. 17). However, as emphasized in Ref. 15, the ''bare'' 5LM without proper far-level contributions is not adequate to describe heavy-hole valence bands, so that its main advantage over the approach of Ogg is lost. In addition, it turns out that the bare 5LM is not good enough to properly account for the experimentally observed anisotropy of the conduction band in GaAs (cf. Ref. 15).

It is the purpose of the present work to overcome these deficiencies by including in 5LM description the main contributions from far levels. In this version, our model generalizes that of Kane and of Pidgeon and Brown from three to five levels. In order to keep the problem tractable, we do not include all far-level contributions allowed by the crystal symmetry, but only the important ones. This amounts to introducing modified Luttinger parameters, resulting from the interaction of the $\Gamma_8^v$ valence level with far levels, and the linear $k$ terms, as they cause qualitatively different band-structure features. Since our present approach is a generalization of our previous work,[15] we refer to it as I and do not repeat many details discussed there. As before, we try to describe various magneto-optical data in order to test the

 

validity of our model for GaAs and InP and to adjust the band parameters for the two materials. In particular, we test the model by comparing the results of the theory with experimental data at megagauss magnetic fields, at which the electrons occupy high energies in the conduction band.

It has been recognized that a resonant electron-optic phonon interaction in medium-gap semiconductors in the presence of a magnetic-field results in effects comparable to those of the band structure.[18,19] As a consequence, aiming at a realistic description of conduction electrons in GaAs and InP, we include resonant and nonresonant polaron effects.

Our paper is organized in the following way. First, we consider the case of no external field, present the $\mathbf{k}\cdot\mathbf{p}$ theory, and describe its results. Next, we turn to magnetic-field effects, present the $\mathbf{P}\cdot\mathbf{p}$ theory, mention resonant polarons, and describe the resulting properties of conduction electrons in GaAs and InP. In the discussion, we compare the resulting band parameters for the valence bands with those proposed by other authors.

## II. FIVE-LEVEL k·p THEORY

We first consider the case of no external fields. The initial one-electron eigenvalue problem reads

$$\left[\frac{\mathbf{p}^2}{2m_0}+V_0(\mathbf{r})+\frac{\hbar}{4m_0^2c^2}\,(\boldsymbol{\sigma}\times\boldsymbol{\nabla}V_0)\cdot\mathbf{p}\right]\Psi=E\Psi, \qquad (1)$$

where $V_0$ is the periodic lattice potential, $m_0$ is the free-electron mass, and the spin-orbit term is written in the standard notation. We look for solutions of (1) in the form of Luttinger and Kohn[5] (LK),

$$\Psi_k^m(\mathbf{r})=\exp(i\mathbf{k}\cdot\mathbf{r})\sum_l c_l^m(k)u_l(\mathbf{r}). \qquad (2)$$

The summation is over all bands and the index $m$ indicates the band of interest. The LK periodic amplitudes satisfy (1) at a band's extremum (at $k=0$ in our case),

$$\left[\frac{\mathbf{p}^2}{2m_0}+V_0(\mathbf{r})+\frac{\hbar}{4m_0^2c^2}\,(\boldsymbol{\sigma}\times\boldsymbol{\nabla}V_0)\cdot\mathbf{p}\right]u_l=E_{l0}u_l, \qquad (3)$$

where $E_{l0}$ is the edge energy of the $l$th band. The LK functions are orthonormal. Inserting (2) into Eq. (1), multiplying on the left by $u_{l'}^*$, and integrating over the unit cell, one obtains

$$\sum_l\left\{\left[E_{l0}+\frac{\hbar^2k^2}{2m_0}-E\right]\delta_{l'l}+\frac{\hbar}{m_0}\,\mathbf{k}\cdot\mathbf{p}_{l'l}+H^{\text{s.o.}}_{l'l}\right\}c_l^m=0. \qquad (4)$$

The index $l'=1,2,3,...$ runs over the bands, and $\mathbf{p}_{l'l}$ are interband matrix elements,

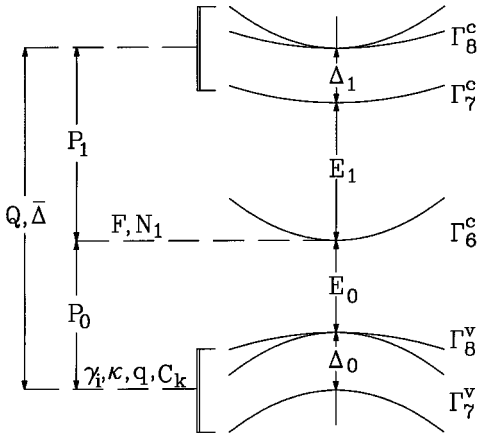


FIG. 1. Five-level model for the conduction and valence bands of GaAs and InP, near the Γ point of the Brillouin zone. The interband matrix elements of momentum and of the spin-orbit interaction, as well as the far-level contributions, are indicated symbolically.

$$\mathbf{p}_{l'l}=\frac{1}{\Omega}\left\langle u_{l'}\left|\mathbf{p}+\frac{\hbar}{4m_0c^2}\,(\boldsymbol{\sigma}\times\boldsymbol{\nabla}V_0)\right|u_l\right\rangle.$$

The second term in the above equation appears to lead to linear $k$ terms in the energy and it has been often cited in the literature in this context. However, as shown by Bir and Pikus,[20] this term vanishes for $l=l'$. There exist other sources of linear $k$ terms (cf. Refs. 21 and 13) and we deal with them below. If the $u_l$ amplitudes satisfy rigorously Eq. (3), the interband spin-orbit terms $H^{\text{s.o.}}_{l'l}$ do not appear in Eq. (4). However, we will use the LK functions, which do not satisfy (3) exactly, so that $H^{\text{s.o.}}_{l'l}$ remain.

In the following, we consider a 5LM of the band structure at $k=0$ (cf. Fig. 1). The set of $u_l$ amplitudes used in the calculations is specified in I. The chosen $u_l$ functions diagonalize the spin-orbit interaction within $(\Gamma_8^c,\Gamma_7^c)$ and $(\Gamma_8^v,\Gamma_7^v)$ multiplets. As a consequence, due to inversion asymmetry of the zinc-blende lattice, there exists a spin-orbit coupling $\Delta$ between the above multiplets [Pollak, Higginbotham, and Cardona (Ref. 22)].

As mentioned in the Introduction, in addition to the five levels, we include far levels (higher and lower) in approximation up to $k^2$ terms. This scheme is due to Lowdin[23] and it has been applied to InSb by Kane.[1] It can be considered as a combination of perturbation theory for quasidegenerate levels (five levels) and nondegenerate levels (far-level contributions). The far-level contributions projected on the five-level scheme (14 states including spin and $\Gamma_8^c$, $\Gamma_8^v$ degeneracies) result in many additional terms involving a large number of parameters. In order to keep the problem tractable, we include the diagonal contributions to the conduction $\Gamma_6^c$ band, the contributions to the Luttinger valence $\gamma^L$ parameters, and the linear $k$ terms. Other far-level terms are neglected.

Taking the LK basis in the order: $u_1$, $u_9$, $u_3$, $u_{11}$, $u_5$, $u_{13}$, $u_7$, $u_8$, $u_2$, $u_{10}$, $u_4$, $u_{12}$, $u_6$, $u_{14}$ (cf. I), the matrix takes the form (5),

$$
\begin{bmatrix}
G_1'-\lambda & 0 & 0 & \sqrt{\tfrac{1}{3}}P_1k_- & \tfrac{1}{3}\overline{\Delta} & \sqrt{\tfrac{1}{3}}Qk_z & 0 & 0 & 0 & 0 & -\sqrt{\tfrac{2}{3}}P_1k_z & 0 & -\sqrt{\tfrac{2}{3}}Qk_- & Qk_+ \\
 & G_1'-\lambda & 0 & -P_1k_+ & -\sqrt{\tfrac{1}{3}}Qk_z & \tfrac{1}{3}\overline{\Delta} & -\sqrt{\tfrac{2}{3}}Qk_z & 0 & 0 & 0 & 0 & -\sqrt{\tfrac{2}{3}}Qk_- & 0 & \sqrt{\tfrac{1}{3}}Qk_- \\
 & & E_1'-\lambda & \sqrt{\tfrac{2}{3}}P_1k_- & 0 & \sqrt{\tfrac{2}{3}}Qk_z & -\tfrac{2}{3}\overline{\Delta} & 0 & 0 & 0 & \sqrt{\tfrac{1}{3}}P_1k_z & -Qk+ & \sqrt{\tfrac{1}{3}}Qk_- & 0 \\
 & & & E_k2F-\lambda & \sqrt{\tfrac{1}{3}}P_0k_+ & -P_0k_- & \sqrt{\tfrac{2}{3}}P_0k_+ & \sqrt{\tfrac{2}{3}}P_1k_z & 0 & -\sqrt{\tfrac{1}{3}}P_1k_z & 0 & \sqrt{\tfrac{2}{3}}P_0k_z & 0 & -\sqrt{\tfrac{1}{3}P_0k_z} \\
 & & & & & & & 0 & \sqrt{\tfrac{2}{3}}Qk_- & -Qk_+ & -\sqrt{\tfrac{2}{3}}P_0k_z & & & \\
 & & & & & S_1 & & \sqrt{\tfrac{2}{3}}Qk_- & 0 & -\sqrt{\tfrac{1}{3}}Qk_- & 0 & & S_3 & \\
 & & & & & & & Qk_+ & -\sqrt{\tfrac{1}{3}}Qk_- & 0 & \sqrt{\tfrac{1}{3}}P_0k_z & & & \\
 & & & & & & & G_1'-\lambda & 0 & 0 & \sqrt{\tfrac{1}{3}}P_1k_+ & \tfrac{1}{3}\overline{\Delta} & \sqrt{\tfrac{1}{3}}Qk_z & 0 \\
 & & & & & & & & G_1'-\lambda & 0 & P_1k_- & -\sqrt{\tfrac{1}{3}}Qk_z & \tfrac{1}{3}\overline{\Delta} & -\sqrt{\tfrac{2}{3}}Qk_z \\
 & & & & & & & & & E_1'-\lambda & \sqrt{\tfrac{2}{3}}P_1k_+ & 0 & \sqrt{\tfrac{2}{3}}Qk_z & -\tfrac{2}{3}\overline{\Delta} \\
 & & & & & & & & & & E_k2F-\lambda & \sqrt{\tfrac{1}{3}}P_0k_- & P_0k_+ & \sqrt{\tfrac{2}{3}}P_0k_- \\
 & & & & & & & & & & & & S_2 &
\end{bmatrix} \tag{5}
$$

where $k_\pm=(k_x\pm ik_y)/\sqrt{2}$ and $\lambda=E-E_k$, in which $E_k=\hbar^2k^2/2m_0$. The parameters $P_0$, $P_1$, and $Q$ are the interband matrix elements of momentum and $\overline{\Delta}$ is that of the spin-orbit interaction (shown schematically in Fig. 1 and defined in I). Due to the appearance of the off-diagonal element $\overline{\Delta}$, the $G_1'$, $E_1'$, $E_0'$, $G_0'$, energies on the diagonal of (5) are not the observable band-edge energies $E_0$, $E_1$, $\Delta_0$, $\Delta_1$ (cf. Fig. 1), but the energies that become the observable ones when the matrix is diagonalized at $k=0$ (cf. I). The zero of energy is taken at the $\Gamma_6^c$ edge. In GaAs and InP, the values of $\Delta$ are small and the energies on the diagonal are close to the observable ones.

Blocks $S_1$, $S_2$, and $S_3$ are given by Eqs. (6), (7), and (8), respectively,

$$
S_1=\begin{bmatrix}
E_0'-E_k(\gamma_1-\gamma_2)-3E_z\gamma_2-E & \sqrt{3}R[(k_x^2-k_y^2)\gamma_2-ik_xk_y2\gamma_3]-C_kk_z & \sqrt{2}\gamma_2(3E_z-E_k) \\
 & E_0'-E_k(\gamma_1+\gamma_2)+3E_z\gamma_2-E & \sqrt{6}R[(k_x^2-k_y^2)\gamma_2+ik_xk_y2\gamma_3] \\
 & & G_0'-E_k\gamma_1-E
\end{bmatrix}, \tag{6}
$$

$$
S_2=\begin{bmatrix}
E_0'-E_k(\gamma_1-\gamma_2)-3E_z\gamma_2-E & \sqrt{3}R[(k_y^2-k_x^2)\gamma_2-ik_xk_y2\gamma_3]-C_kk_z & \sqrt{2}\gamma_2(3E_z-E_k) \\
 & E_0'-E_k(\gamma_1+\gamma_2)+3E_z\gamma_2-E & \sqrt{6}R[(k_y^2-k_x^2)\gamma_2+ik_xk_y2\gamma_3] \\
 & & G_0'-E_k\gamma_1-E
\end{bmatrix}, \tag{7}
$$

$$
S_3=\begin{bmatrix}
-\sqrt{3/2}C_kk_+ & 2\sqrt{6}\,\gamma_3Rk_zk_+-\sqrt{1/2}C_kk_- & 6\,\gamma_3Rk_zk_- \\
2\sqrt{6}\,\gamma_3Rk_zk_++\sqrt{1/2}C_kk_- & -\sqrt{3/2}C_kk_+ & -2\sqrt{3}\,\gamma_3Rk_zk_+ \\
-6\,\gamma_3Rk_zk_- & -2\sqrt{3}\,\gamma_3Rk_zk_+ & 0
\end{bmatrix}, \tag{8}
$$

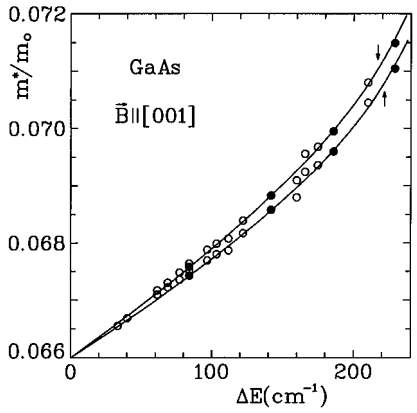


FIG. 2. Cyclotron masses of electrons in GaAs versus transition energy (spin-up and spin-down transitions) for $\mathbf{B}\|[001]$. The solid lines are calculated. Experimental data: open circles, Hopkins *et al.* (Ref. 16); solid circles, Sigg *et al.* (Ref. 34).

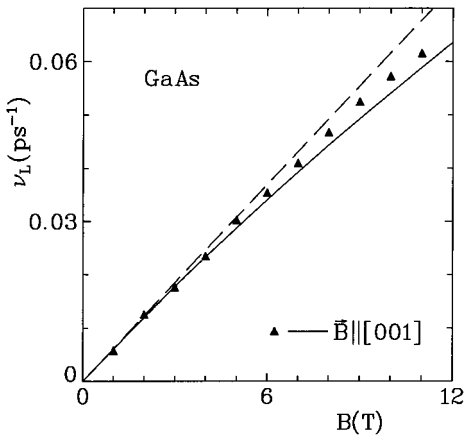


FIG. 3. The Larmor frequency for the conduction electrons in GaAs versus magnetic field. Experimental data are after Hannak *et al.* (Ref. 33), the solid line is calculated. The dashed straight line corresponds to the constant Landé factor $g^*=-0.44$.

where $R=\hbar^2/2m_0$, $E_z=\hbar^2k_z^2/2m_0$, and $C_k$ represent linear $k$ terms. Quantities $\gamma_i$ represent modified Luttinger parameters, in which the $\mathbf{k}\cdot\mathbf{p}$ interaction of the $\Gamma_8^v$ level with the $\Gamma_6^c$, $\Gamma_8^c$, $\Gamma_7^c$ levels has been subtracted, since it is included explicitly in the matrix (5). (We include here also the parameter $\kappa$, appearing later in the magnetic-field problems.) Thus, we have

$$\begin{aligned}
\gamma_1&=\gamma_1^L+\frac{E_{P_o}}{3E_0}-\frac{E_Q}{3(E_1-E_0)}-\frac{E_Q}{3(E_1+\Delta_1-E_0)},\\
\gamma_2&=\gamma_2^L+\frac{E_{P_o}}{6E_0}+\frac{E_Q}{6(E_1-E_0)},\\
\gamma_3&=\gamma_3^L+\frac{E_{P_o}}{6E_0}-\frac{E_Q}{6(E_1-E_0)},\\
\kappa&=\kappa^L+\frac{E_{P_o}}{6E_0}+\frac{E_Q}{18(E_1-E_0)}+\frac{E_Q}{9(E_1+\Delta_1-E_0)}.
\end{aligned}\tag{9}$$

The terms related to $F$, $\gamma_i$, and $C_k$ represent far-level contributions (in I, we used the parameter $C=2F$). Our parameter $F$ is not identical with that appearing in the three-level model. Relations (9) neglect small terms related to $\Delta$.

The $\mathbf{k}\cdot\mathbf{p}$ theory in the above form contains three kinds of parameters: the energy gaps, the matrix elements of momentum and of the spin-orbit interaction, and the combinations of both. In the following, we use the values of energy gaps $E_0$, $\Delta_0$, $E_1$, $\Delta_1$ measured experimentally and the values of $\Delta$ and $C_k$ calculated theoretically by independent methods. Other parameters are determined by fitting various experimental data, as described below. The linear $k$ terms (proportional to $C_k$) result in very small effects, so that they may be neglected in most calculations.

## III. NONRESONANT POLARONS

In polar materials GaAs and InP, one deals with resonant and nonresonant effects of the electron-phonon interaction (polarons). The influence of resonant polaron on electron properties is discussed below in sections concerned with the presence of an external magnetic field. The nonresonant polaron affects the band-edge effective mass according to the relation[19]

$$m_0^*(\exp)=m_{\rm pol}^*=m_0^*\,\frac{(1+\alpha/2)}{(1+\alpha/3)},\tag{10}$$

where $\alpha$ is the polar coupling constant. Knowing the value of $\alpha$ and the experimentally measured mass $m_0^*(\exp)$, one determines the bare mass $m_0^*$, which is then used in the band-structure calculations. Finally, the polaron correction is put back to retrieve the experimental mass value. In the following section, dealing with the band structure at $B=0$, we perform the calculations for two values of the polar constant: $\alpha=0.065$ and 0.085. The first is the usually accepted value (cf. Ref. 18). We find, however, that some important data are described better if the bare electron mass is determined with the use of the second value. The same problem appears in InP, the corresponding values of the polar constant are $\alpha=0.12$ and 0.20. This question is considered in the Discussion.

## IV. k·p THEORY. RESULTS

In this section, we quote the band parameters and describe the results of the $\mathbf{k}\cdot\mathbf{p}$ theory for GaAs and InP. Although we are concerned here with the band structure at $B=0$, one should bear in mind that the precise magneto-optical experiments quoted in the following sections are of decisive importance for the adjustment of band parameters.

### A. GaAs

We use the following experimental energy gaps: $E_0=-1.519$ eV, $\Delta_0=-0.341$ eV, $E_1=2.969$ eV, $\Delta_1=0.171$ eV, $\Delta=-0.061$ eV (cf. I), and $C_k=-3.4$ meV Å (cf. Ref. 13). The effective mass and the effective spin $g$ value at the conduction-band edge are,

$$m_0^*(\exp)=0.066m_0,\quad g_0^*=-0.44,\tag{11}$$

as determined by the cyclotron resonance (cf. Fig. 2), and the spin resonance[24] (cf. also Fig. 3).

For the polar constant $\alpha=0.065$ the bare electron mass at the band edge is $m_0^*=0.0653m_0$, while for $\alpha=0.085$, there is

TABLE I. Far-band parameters for GaAs, adjusted to fit the experimental data for two values of the polar constant $\alpha$.

| | $\gamma_1$ | $\gamma_2$ | $\gamma_3$ | $\kappa$ | $N_1$ | $q$ | $F$ |
|---|---|---|---|---|---|---|---|
| $\alpha$=0.065 | 0.176 | 0.421 | 0.105 | 0.616 | −0.0107 | 0.01 | −1.075 |
| $\alpha$=0.085 | −0.586 | −0.021 | −0.336 | −0.465 | −0.0105 | 0.01 | −1.055 |

$m_0^*=0.0651m_0$. The adjusted values of the interband matrix elements for the both cases are

$$E_{P_0}=27.86\ \text{eV},\quad E_{P_1}=2.36\ \text{eV},\quad E_Q=15.56\ \text{eV}, \tag{12}$$

in the standard units of $E_P=2m_0P^2/\hbar^2$. The adjusted values of other band parameters for the two cases are quoted in Table I. (The parameters $N_1$ and $q$ are related to the band structure in the presence of magnetic field, see below. Our value of $N_1$ is not identical with that appearing in the three-level model. In I, we used the parameter $C'=2N_1$.)

Using the matrices (5)–(8), we calculate $E(\mathbf{k})$ dispersions for the seven bands in question. The resulting conduction band is nonparabolic, nonspherical, and spin split (for a given direction of $\mathbf{k}$). The nonsphericity is related to the $Q$ terms and the difference between $\gamma_2$ and $\gamma_3$ values. The spin splitting, which is in general due to the lack of inversion symmetry in zinc-blende crystals, is related specifically to the nonzero values of $P_1$ and $\Delta$ (which vanish for crystals with inversion symmetry).

We illustrate our calculations in Fig. 4, which shows the electron velocities $\mathbf{v}(\mathbf{k})=\partial E/\partial\hbar\mathbf{k}$ for $\mathbf{k}\|$ to the three principal crystal directions. The velocity maxima correspond to inflection points of $E(\mathbf{k})$ dispersion. In the calculations of velocity, we have neglected small effects of the spin splitting (cf. below). The dispersions $E(\mathbf{k})$ for $\mathbf{k}$ parallel to the main crystal directions and the corresponding effective masses have been shown explicitly in I. Our present calculation gives very similar results for the conduction band. Also, the explicit formula for the band-edge electron mass obtained in the ''bare'' 5LM model [cf. I, Eq. (12)] remains valid.

In order to describe analytically the band nonparabolicity and to facilitate calculations, which do not require a high precision, we introduce an effective two-level formula,

$$\frac{\hbar^2k^2}{2m_0^*}=E\left(1+\frac{E}{E_0^*}\right), \tag{13}$$

in which $m_0^*=m_0^*(\text{exp})$ and the effective value of $E_0^*$ is adjusted to fit the mean $E(\mathbf{k})$ value at $k=5.5\times10^6\ \text{cm}^{-1}$, averaged over the three $\mathbf{k}$ directions (values for $\mathbf{k}\|[001]$ and $\mathbf{k}\|[111]$ are counted twice, as they are spin degenerate). Our calculated value of the ''effective'' gap is $E_0^*=0.98$ eV. It indicates that the conduction band in GaAs is considerably more nonparabolic than it would follow from a two-level $\mathbf{k}\cdot\mathbf{p}$ model with the real gap $E_g=1.52$ eV. In other words, it demonstrates the necessity of the five-level model. Equation (13) is easily applicable to various observable properties and it has been extensively used to describe the two-dimensional electron gas in GaAs-$Ga_xAl_{1-x}As$ heterostructures. These descriptions confirmed the effective gap value (cf. Discussion). In the effective two-level description (13), the momentum mass $1/m^*=(1/\hbar^2k)\partial E/\partial k$, defined by the relation $m^*\mathbf{v}=\hbar\mathbf{k}$, is given by the formula $m^*(E)=m_0^*(1+2E/E_0^*)$ (cf. Ref. 25).

The calculated dispersion relation for the conduction band exhibits a spin splitting. This splitting is due to the lack of inversion symmetry and it obeys the relation $E_\downarrow(\mathbf{k})=E_\uparrow(-\mathbf{k})$. The splitting at low $k$ values is proportional to $k^3$ (cf. I). The explicit expression for the spin-splitting parameter $\gamma$ is obtained by perturbation theory of the third order. The result is

$$\gamma=\frac{4}{3}\frac{Q}{E_0E_1G_0G_1}\left[P_0P_1(E_0'E_1'-G_0'G_1')-\frac{\overline{\Delta}}{3}[P_0^2(2G_1'+E_1')-P_1^2(2E_0'+G_0')]\right]+\gamma_c, \tag{14}$$

where

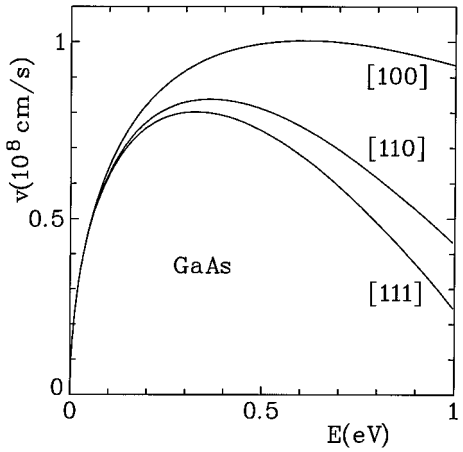


FIG. 4. The electron velocity in the conduction band of GaAs versus the electron energy, as calculated for $\mathbf{k}$ parallel to the principal crystal directions.

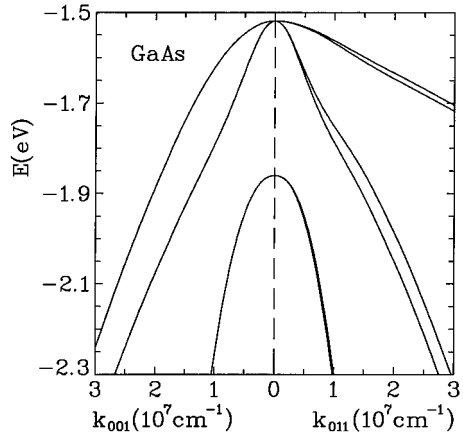


FIG. 5. The dispersion relations $E(\mathbf{k})$ for the valence bands of GaAs, calculated for two $\mathbf{k}$ directions. The corresponding hole masses are quoted in Tables II and III.

$$\gamma_c = -\frac{C_k}{\sqrt{3}}\left[\frac{3P_0(G_1'-E_0)-P_1\overline{\Delta}}{3E_0(G_1-E_0)}\right]^2. \qquad (15)$$

The contribution of $C_k$ terms to the spin splitting of the conduction band is small. Using our parameters for GaAs, we calculate $\gamma=24.21$ eV Å$^3$ and $\gamma_c=0.09$ eV Å$^3$. The value of $\gamma$ is in good agreement with experimental estimations (cf. the discussion in I). It can be seen from (14) that the sign of $\Delta$ is of importance for the value of $\gamma$. In GaAs the sign of $\Delta$ is negative and we deal with the sum of the two terms in square parenthesis of (14). The term proportional to $\Delta$ contributes about one third of the total value of $\gamma$.

In Fig. 5, we show the calculated dispersion relations for light-hole, heavy-hole, and split-off valence bands for $\mathbf{k}\|[001]$ and $\mathbf{k}\|[011]$ crystal directions. The light-hole band is seen to be strongly spin split for $\mathbf{k}\|[011]$. The splitting of all bands vanishes for $\mathbf{k}\|[001]$. In contrast to the bare 5LM model described in I, our present treatment aims at a realistic description of the heavy-hole bands. The calculated light-hole, heavy-hole, and split-off band masses are quoted in Tables II and III (cf. Discussion) and compared to the calculated and experimental values of other authors.

Finally, the linear $k$ terms in the matrix (5) result in the splitting of the $\Gamma_8$ valence bands away from $k=0$. In GaAs,

TABLE II. Luttinger parameters for the valence bands of GaAs and the resulting heavy and light masses for two **k** directions, as calculated or measured by various authors. The values determined in this work for two polar constants are given at the end.

| | $\gamma_1^L$ | $\gamma_2^L$ | $\gamma_3^L$ | $\kappa^L$ | $m_{\rm hh}^{100}/m_0$ | $m_{\rm lh}^{100}/m_0$ | $m_{\rm hh}^{111}/m_0$ | $m_{\rm lh}^{111}/m_0$ |
|---|---|---|---|---|---|---|---|---|
| Pollak *et al.*[a] | 7.39 | 2.47 | 2.87 | | 0.40 | 0.081 | 0.61 | 0.076 |
| Vrehen[b] | 7.2 | 2.5 | 2.5 | | 0.45 | 0.082 | 0.45 | 0.082 |
| Bowers and Mahan[c] | 5.80 | 1.22 | 1.95 | | 0.30 | 0.122 | 0.52 | 0.10 |
| Balslev[d] | 6.77 | 2.28 | 2.88 | | 0.45 | 0.088 | 0.99 | 0.080 |
| Lawaetz[e] | 7.65 | 2.41 | 3.28 | 1.72 | 0.35 | 0.080 | 0.92 | 0.070 |
| Seisyan *et al.*[f] | 7.1 | 2.32 | 2.54 | | 0.41 | 0.085 | 0.50 | 0.082 |
| Lawaetz[g] | 7.98 | 2.58 | 3.20 | | 0.35 | 0.076 | 0.63 | 0.070 |
| Skolnick *et al.*[h] | 6.98 | 2.25 | 2.88 | | 0.40 | 0.087 | 0.82 | 0.078 |
| Hess *et al.*[i] | 6.85 | 2.10 | 2.90 | | 0.38 | 0.090 | 0.95 | 0.070 |
| Bimberg[j] | 6.85 | 2.1 | 2.9 | 1.2 | 0.38 | 0.090 | 0.95 | 0.079 |
| Ekardt *et al.*[k] | 7.05 | 2.35 | 3.0 | 1.28 | 0.43 | 0.085 | 0.95 | 0.077 |
| Miller *et al.*[l] | 6.8 | 1.9 | | | 0.33 | 0.094 | | |
| Hayakawa *et al.*[m] | 4.8 | | 1.85 | | | | 0.90 | 0.117 |
| Hayakawa *et al.*[m] | 5.74 | 1.39 | | | 0.34 | 0.117 | | |
| Neumann *et al.*[n] | 7.17 | 2.88 | 2.91 | 1.81 | 0.71 | 0.077 | 0.74 | 0.077 |
| Molenkamp *et al.*[o] | 6.79 | 1.924 | 2.681 | | 0.34 | 0.094 | 0.70 | 0.082 |
| Shanabrook *et al.*[p] | 6.8 | 1.9 | 2.73 | | 0.34 | 0.094 | 0.75 | 0.082 |
| Said and Kanehisa[q] | 7.20 | 2.15 | 3.05 | | 0.34 | 0.087 | 0.91 | 0.075 |
| Binggeli *et al.*[r] | 7.10 | 2.02 | 2.91 | | 0.33 | 0.090 | 0.78 | 0.077 |
| $\alpha=0.065$ | 8.56 | 2.90 | 3.74 | 3.11 | 0.36 | 0.070 | 0.93 | 0.062 |
| $\alpha=0.085$ | 7.80 | 2.46 | 3.30 | 2.03 | 0.35 | 0.079 | 0.83 | 0.069 |

[a]F. H. Pollak, C. W. Higginbotham, and M. Cardona, J. Phys. Jpn. Suppl. **21**, 20 (1966).
[b]Q. H. Vrehen, J. Phys. Chem. Solids **29**, 129 (1968).
[c]R. L. Bowers and G. D. Mahan, Phys. Rev. **185**, 1073 (1969).
[d]I. Balslev, Phys. Rev. **177**, 1173 (1969).
[e]P. Lawaetz, Phys. Rev. B **4**, 3460 (1971).
[f]R. P. Seisyan, M. A. Abdullaev, and V. D. Drazin, Fiz. Tekh. Poluprovodn. **7**, 522 (1993) [Sov. Phys. Semicond. **7**, 522 (1973)].
[g]P. Lawaetz, J. Phys. C **9**, 2809 (1976).
[h]M. S. Skolnick *et al.*, J. Phys. C **9**, 2809 (1976).
[i]K. Hess *et al.*, *Proceedings of the 13th International Conference on Physics of Semiconductors, Rome, 1976*, edited by F. G. Fumi (North-Holland, Amsterdam, 1976), p. 142.
[j]D. Bimberg, *Advances in Solid State Physics*, edited by J. Treusch (Vieweg, Braunschweig, 1977), Vol. XVII, p. 195.
[k]W. Ekardt, K. Losch, and D. Bimberg, Phys. Rev. B **20**, 3303 (1979).
[l]R. C. Miller, D. A. Kleinman, and A. C. Gossard, Phys. Rev. B **29**, 7085 (1984).
[m]T. Hayakawa *et al.*, Phys. Rev. Lett. **60**, 349 (1988); Phys. Rev. B **38**, 1526 (1988).
[n]Ch. Neumann, A. Nothe, and N. O. Lipari, Phys. Rev. B **37**, 922 (1988).
[o]L. W. Molenkamp *et al.*, Phys. Rev. B **38**, 4314 (1988).
[p]B. V. Shanabrook, O. J. Glembocki, D. A. Broido, and W. I. Wang, Phys. Rev. B **39**, 3411 (1989).
[q]M. Said and Kanehisa, Phys. Status Solidi B **157**, 311 (1990).
[r]N. Binggeli and A. Baldereschi, Phys. Rev. B **43**, 14734 (1991).

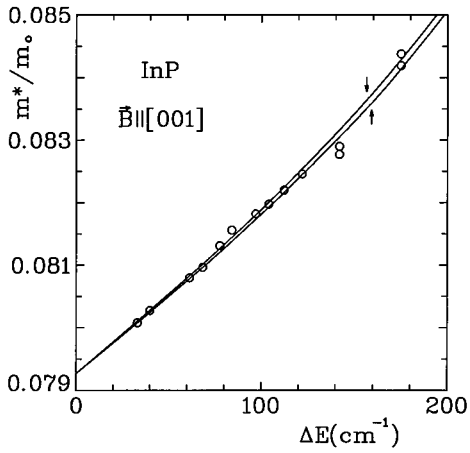


FIG. 6. Cyclotron masses of electrons in InP versus transition energy (spin-up and spin-down transitions) for **B**||[001]. The solid lines are calculated. Experimental data: circles, Hopkins *et al.* (Ref. 16).

this effect is very weak: the valence maxima occur at $k=6\times10^4$ cm$^{-1}$ for **k**||[111] and they are $1.4\times10^{-3}$ meV higher than the $\Gamma_8$ point.

### B. InP

We use the following experimental energy gaps: $E_0=-1.423$ eV, $\Delta_0=-0.108$ eV, $E_1=3.297$ eV, and $\Delta_1=0.201$ eV (cf. Ref. 16). Further, we take $\Delta=0.08733$ eV, calculated by Gorczyca, Pfeffer, and Zawadzki[26] (note the difference of sign in comparison with GaAs) and $C_k=-14.4$ meV Å (cf. Ref. 13).

The experimental values of the electron effective mass and the electron $g^*$ factor are

$$m_0^*(\text{exp})=0.079\ 27m_0, \quad g_0^*=1.26, \tag{16}$$

as determined by the cyclotron resonance (cf. Fig. 5 of Ref. 16 and our Fig. 6) and the spin resonance (cf. Ref. 17). Again, we consider two different values of the polar coupling constant: $\alpha=0.12$ (cf. Refs. 27 and 28) and $\alpha=0.20$. For $\alpha=0.12$, the bare band-edge mass is $m_0^*=0.0778m_0$, while for $\alpha=0.20$ one gets $m_0^*=0.0769m_0$. The adjusted values of the interband matrix elements for the both cases are

$$E_{P_0}=20.93\ \text{eV}, \quad E_{P_1}=0.165\ \text{eV}, \quad E_Q=15.56\ \text{eV}, \tag{17}$$

in the standard units. The adjusted values of other band parameters are quoted in Table IV. As in the case of GaAs, the resulting energy bands of InP are nonparabolic, nonspherical, and spin split. The effective gap value, characterizing the calculated conduction-band nonparabolicity according to the two-level formula (13), is $E_0^*=0.89$ eV, demonstrating the necessity of the 5LM for InP. For the spin splitting of the conduction band, due to inversion asymmetry, we calculate $\gamma=-7.55$ eV Å$^3$ and $\gamma_c=0.33$ eV Å$^3$. The value of $\gamma$ is in good agreement with the experimental estimation [7.26–9.5 eV Å$^3$ (Ref. 29), the sign of $\gamma$ is not determined]. In InP, the value of $\Delta$ is positive (cf. Refs. 26 and 13), so that in square parenthesis of Eq. (14), one deals with the difference of the two terms. In fact, the term proportional to $\Delta$ dominates, so that the sign of $\gamma$ becomes negative.

In Fig. 7, we show the calculated dispersion relations for the valence bands, qualitatively similar to those in GaAs. The calculated effective masses are quoted in Tables V and VI (cf. Discussion). The splitting of the valence $\Gamma_8$ bands resulting from the linear $k$ terms is very small: the maxima of the valence band occur at $k=1.53\times10^5$ cm$^{-1}$ for **k**||[111] and they are $1.55\times10^{-2}$ meV higher than the $\Gamma_8$ point.

TABLE III. Hole mass of the split-off $\Gamma_7^v$ valence band of GaAs, as calculated or measured by various authors. The values determined in this work for two polar constants are given at the end.

| | $m_{so}/m_0$ |
|---|---|
| Ehrenreich[a] | 0.2 |
| Braunstein and Kane[b] | 0.388 |
| Walton and Mishra[c] | 0.133 |
| Vrehen[d] | 0.159 |
| Narita *et al.*[e] | 0.185 |
| Reine *et al.*[f] | 0.154 |
| Lawaetz[g] | 0.15 |
| Molenkamp *et al.*[h] | 0.15 |
| Cardona *et al.*[i] | 0.18 |
| Cardona *et al.*[i] | 0.20 |
| Belov *et al.*[j] | 0.156 |
| $\alpha=0.065$ | 0.138 |
| $\alpha=0.085$ | 0.154 |

[a]H. Ehrenreich, Phys. Rev. **120**, 1951 (1960).
[b]R. Braunstein and E. O. Kane, J. Phys. Chem. Solids **23**, 1423 (1962).
[c]A. K. Walton and U. K. Mishra, J. Phys. C **1**, 533 (1968).
[d]Q. H. Vrehen, J. Phys. Chem. Solids **29**, 129 (1968).
[e]S. Narita, M. Kobayashi, and N. Koike, *Proceedings of the 9th International Conference on the Physics of Semiconductors, Moscow, 1968*, edited by S. M. Ryvkin (Nauka, Leningrad, 1968), p. 347.
[f]M. Reine, R. L. Aggarwal, B. Lax, and C. M. Wolfe, Phys. Rev. B **2**, 458 (1970).
[g]P. Lawaetz, Phys. Rev. B **4**, 3460 (1971).
[h]L. W. Molenkamp *et al.*, Phys. Rev. B **38**, 4314 (1988).
[i]Reference 13.
[j]N. P. Belov, V. T. Prokopenko, and A. D. Yas'kov, Fiz. Tekh. Poluprovodn. **23**, 2093 (1989) [Sov. Phys. Semicond. **23**, 1296 (1989)].

TABLE IV. Far-band parameters for InP, adjusted to fit the experimental data for two values of the polar constant $\alpha$.

| | $\gamma_1$ | $\gamma_2$ | $\gamma_3$ | $\kappa$ | $N_1$ | $q$ | $F$ |
|---|---|---|---|---|---|---|---|
| $\alpha=0.12$ | 0.444 | 0.458 | −0.131 | 1.083 | −0.022 | 0.02 | −1.23 |
| $\alpha=0.20$ | −0.496 | −0.152 | −0.681 | 0.163 | −0.022 | 0.02 | −1.15 |

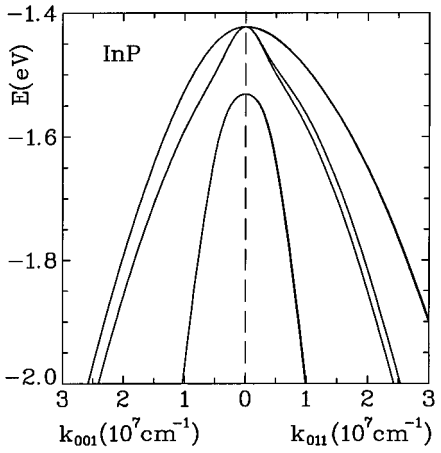


FIG. 7. The dispersion relations $E(\mathbf{k})$ for the valence bands of InP, calculated for two $\mathbf{k}$ directions. The corresponding hole masses are quoted in Tables V and VI.

## V. P·p THEORY

The initial one-electron eigenvalue problem for an electron in a periodic potential and an external magnetic field reads

$$\left[\frac{\mathbf{P}^2}{2m_0}+V_0(\mathbf{r})+\frac{\hbar}{4m_0^2c^2}\,(\boldsymbol{\sigma}\times\boldsymbol{\nabla}V_0)\cdot\mathbf{P}+\mu_B\mathbf{B}\cdot\boldsymbol{\sigma}\right]\Psi=E\Psi, \tag{18}$$

where $\mathbf{P}=\mathbf{p}+e\mathbf{A}$ is the kinetic momentum, $\mathbf{A}$ is the vector potential of magnetic field $\mathbf{B}$, and the Pauli term is written in the standard notation. Due to the presence of a magnetic field, the eigenvalue problem (18) is not periodic. We look for its solutions in the form

$$\Psi=\sum_l f_l(\mathbf{r})u_l(\mathbf{r}), \tag{19}$$

in which $u_l(\mathbf{r})$ are the Luttinger-Kohn periodic functions satisfying (3), and $f_l(\mathbf{r})$ are the envelope functions slowly varying within the unit cell. The summation is over all energy bands. Inserting (19) into (18), using (3), multiplying on the left by $(1/\Omega)u_{l'}^*$, and integrating over the unit cell, one obtains

$$\sum_l\left[\left(\frac{P^2}{2m_0}+E_{l0}-E\right)\delta_{l'l}+\frac{\mathbf{p}_{l'l}\cdot\mathbf{P}}{2m_0}+\mu_B\mathbf{B}\cdot\boldsymbol{\sigma}_{l'l}+H_{l'l}^{\text{s.o.}}\right]f_l=0, \tag{20}$$

where $\boldsymbol{\sigma}_{l'l}=(1/\Omega)\langle u_{l'}|\boldsymbol{\sigma}|u_l\rangle$.

Equation (20) represents a set of coupled differential equations for the envelope functions $f_l$. It involves as yet no approximations, apart from the requirement of slow variation of $\mathbf{A}(\mathbf{r})$ and $f_l(\mathbf{r})$ within the unit cell. We proceed as in the no-field case, specifying the five-level model and taking the basis set of LK functions given in I. Far-band contributions are included using the perturbation theory up to the $P^2$ terms according to the Lowdin procedure. We consider an arbitrary magnetic-field direction in the plane (110), following the procedure of Weiler, Aggarwal, and Lax.[10] The resulting eigenvalue problem takes the form

$$\sum_{l=1}^{14}(\hat{H}_{l'l}^a+\hat{H}_{l'l}^b-E\,\delta_{l'l})f_l=0\quad(l'=1,\ldots,14), \tag{21}$$

TABLE VI. Hole mass of the split-off $\Gamma_7^v$ valence band of InP, as calculated or measured by various authors. The values determined in this work for two polar constants are given at the end.

| | $m_{so}/m_0$ |
|---|---|
| Lawaetz[a] | 0.17 |
| Rochon and Fortin[b] | 0.21 |
| Cardona *et al.*[c] | 0.20 |
| Cardona *et al.*[c] | 0.18 |
| $\alpha=0.12$ | 0.139 |
| $\alpha=0.20$ | 0.162 |

[a]P. Lawaetz, Phys. Rev. B **4**, 3460 (1971).
[b]P. Rochon and E. Fortin, Phys. Rev. B **12**, 5803 (1975).
[c]Reference 13.

TABLE V. Luttinger parameters for the valence bands of InP and the resulting heavy and light masses for two $\mathbf{k}$ directions, as calculated or measured by various authors. The values determined in this work for two polar constants are given at the end.

| | $\gamma_1^L$ | $\gamma_2^L$ | $\gamma_3^L$ | $\kappa^L$ | $m_{\text{hh}}^{100}/m_0$ | $m_{\text{lh}}^{100}/m_0$ | $m_{\text{hh}}^{111}/m_0$ | $m_{\text{lh}}^{111}/m_0$ |
|---|---|---|---|---|---|---|---|---|
| Bowers and Mahan[a] | 5.75 | 1.39 | 2.05 | | 0.34 | 0.117 | 0.61 | 0.101 |
| Lawaetz[b] | 6.28 | 2.08 | 2.76 | 1.47 | 0.47 | 0.096 | 1.32 | 0.085 |
| Leotin *et al.*[c] | 5.04 | 1.56 | 1.73 | | 0.52 | 0.123 | 0.63 | 0.118 |
| Rochon and Fortin[d] | 5.15 | 0.94 | 1.62 | 0.12 | 0.31 | 0.142 | 0.524 | 0.12 |
| Bimberg *et al.*[e] | 4.95 | 1.65 | 2.35 | | 0.61 | 0.121 | 4.0 | 0.104 |
| Ekardt *et al.*[f] | 4.95 | 1.85 | 2.55 | 0.97 | 0.80 | 0.116 | | 0.100 |
| Cardona *et al.*[g] | 5.05 | 1.6 | 1.73 | | 0.54 | 0.121 | 0.63 | 0.117 |
| $\alpha=0.12$ | 7.5 | 2.36 | 2.87 | 3.0 | 0.36 | 0.082 | 0.57 | 0.075 |
| $\alpha=0.20$ | 6.56 | 1.75 | 2.32 | 2.08 | 0.33 | 0.099 | 0.52 | 0.089 |

[a]R. L. Bowers and G. D. Mahan, Phys. Rev. **185**, 1073 (1969).
[b]P. Lawaetz, Phys. Rev. B **4**, 3460 (1971).
[c]J. Leotin *et al.*, Solid State Commun. **15**, 693 (1974).
[d]P. Rochon and E. Fortin, Phys. Rev. B **12**, 5803 (1975).
[e]D. Bimberg *et al.*, Physica **89B**, 139 (1977).
[f]W. Ekardt, K. Losch, and D. Bimberg, Phys. Rev. B **20**, 3303 (1979).
[g]Reference 13.

$$
\begin{bmatrix}
G_1'+\mathscr{E}+\frac{\mu}{3} & 0 & -\frac{\sqrt{8}}{3}\mu & \sqrt{\frac{1}{3}}P_1'P_- & \frac{1}{3}\bar{\Delta} & 0 & 0 & 0 & 0 & 0 & -\sqrt{\frac{2}{3}}P_1'P_z & 0 & 0 & 0 \\
 & G_1'+\mathscr{E}-\mu & 0 & -P_1'P_+ & 0 & \frac{1}{3}\bar{\Delta} & 0 & 0 & 0 & 0 & 0 & 0 & 0 & 0 \\
 & & E_1'+\mathscr{E}-\frac{\mu}{3} & \sqrt{\frac{2}{3}}P_1'P_- & 0 & 0 & -\frac{2}{3}\bar{\Delta} & 0 & 0 & 0 & \sqrt{\frac{1}{3}}P_1'P_z & 0 & 0 & 0 \\
 & & & \mathscr{E}(1+2F) & \sqrt{\frac{1}{3}}P_0'P_+ & -P_0'P_- & \sqrt{\frac{2}{3}}P_0'P_+ & \sqrt{\frac{2}{3}}P_1'P_z & 0 & -\sqrt{\frac{1}{3}}P_1'P_z & 0 & \sqrt{\frac{2}{3}}P_0'P_z & 0 & -\sqrt{\frac{1}{3}}P_0'P_z \\
 & & & -\mu(2N_1+1) & & & & & & & & & & \\
 & & & & & & & 0 & 0 & 0 & -\sqrt{\frac{2}{3}}P_0'P_z & 0 & 2\gamma'''\sqrt{6\mu E_z}a^+ & 6\gamma'''\sqrt{\mu E_z}a \\
 & & & & & M_1 & & 0 & 0 & 0 & 0 & 2\gamma'''\sqrt{6\mu E_z}a^+ & 0 & -2\gamma'''\sqrt{3\mu E_z}a \\
 & & & & & & & 0 & 0 & 0 & \sqrt{\frac{1}{3}}P_0'P_z & -6\gamma'''\sqrt{\mu E_z}a & -2\gamma'''\sqrt{3\mu E_z}a^+ & 0 \\
 & & & & & & G_1'+\mathscr{E}-\frac{\mu}{3} & 0 & \frac{\sqrt{8}}{3}\mu & \sqrt{\frac{1}{3}}P_1'P_+ & \frac{1}{3}\bar{\Delta} & 0 & 0 \\
 & & & & & & & G_1'+\mathscr{E}+\mu & 0 & P_1'P_- & 0 & \frac{1}{3}\bar{\Delta} & 0 \\
 & & & & & & & & E_1'+\mathscr{E}+\frac{\mu}{3} & \sqrt{\frac{2}{3}}P_1'P_+ & 0 & 0 & -\frac{2}{3}\bar{\Delta} \\
 & & & & & & & & & \mathscr{E}(1+2F) & \sqrt{\frac{1}{3}}P_0'P_- & P_0'P_+ & \sqrt{\frac{2}{3}}P_0'P_- \\
 & & & & & & & & & +2\mu(N_1+1) & & & \\
 & & & & & & & & & & & M_2 &
\end{bmatrix}
\tag{22}
$$

in which $\hat{H}^a_{l'l}$ is given by Eq. (22) and the blocks $M_1$ and $M_2$ by Eqs. (23) and (24).

$$
M_1=\begin{bmatrix}
E_0'-\mathscr{E}(\gamma_1-\gamma')-3\gamma' E_z-\mu\kappa-q_5 & 2\sqrt{3}\mu\gamma'' aa & -\sqrt{2}\gamma'(\mathscr{E}-3E_z)-\sqrt{2}\mu(\kappa+1) \\
 & E_0'-\mathscr{E}(\gamma_1+\gamma')+3\gamma' E_z+3\mu\kappa-q_1 & 2\sqrt{6}\gamma'' a^+a^+ \\
 & & G_0'-\mathscr{E}\gamma_1-\mu(1+2\kappa)
\end{bmatrix},
\tag{23}
$$

$$
M_2=\begin{bmatrix}
E_0'-\mathscr{E}(\gamma_1-\gamma')-3\gamma' E_z+\mu\kappa+q_5 & -2\sqrt{3}\mu\gamma'' a^+a^+ & -\sqrt{2}\gamma'(\mathscr{E}-3E_z)+\sqrt{2}\mu(\kappa+1) \\
 & E_0'-\mathscr{E}(\gamma_1+\gamma')+3\gamma' E_z-3\mu\kappa+q_1 & -2\sqrt{6}\gamma'' aa \\
 & & G_0'-\mathscr{E}\gamma_1+\mu(1+2\kappa)
\end{bmatrix}.
\tag{24}
$$

Here $P_0'=P_0/\hbar$, $P_1'=P_1/\hbar$, $\mathscr{E}=2\mu(a^+a+\frac{1}{2})+E_z$, and $\mu=e\hbar B/2m_0$. The operators $P_\pm=(P_x\pm iP_y)/\sqrt{2}$ are proportional to the raising and lowering operators $a^+$ and $a$ for the harmonic-oscillator functions: $P_+=-(\hbar/L)a^+$ and $P_-=-(\hbar/L)a$, in which $L=(\hbar/eB)^{1/2}$ is the magnetic radius.

The matrix $H^b_{l'l}$ is given by Eq. (25),

$$\begin{bmatrix}
0 & 0 & 0 & 0 & & & & 0 & 0 & 0 & 0 & & & \\
 & 0 & 0 & 0 & & A_1 & & 0 & 0 & 0 & 0 & & D & \\
 & & 0 & 0 & & & & 0 & 0 & 0 & 0 & & & \\
 & & & 0 & 0 & 0 & 0 & 0 & 0 & 0 & 0 & 0 & 0 & 0 \\
 & & & & -\mu_1-q_5-i3c_1 & \mu_2^\dagger-q_2+ic_2^\dagger & \sqrt{2}\mu_1^\dagger+ic_6^\dagger & & & & 0 & -q_6-i\sqrt{3}c_3^\dagger & \mu_3+q_3+ic_3 & \sqrt{\tfrac{3}{2}}\mu_3^\dagger+i\sqrt{3}c_7^\dagger \\
 & & & & & \mu_1-q_1-ic_1 & \sqrt{2}\mu_2+ic_5 & & -D & & 0 & \mu_3-q_3-ic_3 & q_4+ic_4 & -\sqrt{\tfrac{1}{2}}\mu_3-ic_7 \\
 & & & & & & 0 & & & & 0 & -\sqrt{\tfrac{3}{2}}\mu_3^\dagger+i\sqrt{3}c_7^\dagger & -\sqrt{\tfrac{1}{2}}\mu_3+ic_7 & 0 \\
 & & & & & & & 0 & 0 & 0 & 0 & & & \\
 & & & & & & & & 0 & 0 & 0 & & A_2 & \\
 & & & & & & & & & 0 & 0 & & & \\
 & & & & & & & & & & 0 & 0 & 0 & 0 \\
 & & & & & & & & & & & -\mu_1+q_5+i3c_1 & -\mu_2-q_2-ic_2 & \sqrt{2}\mu_1^\dagger+ic_6^\dagger \\
 & & & & & & & & & & & & \mu_1+q_1+ic_1 & -\sqrt{2}\mu_2^\dagger-ic_5^\dagger \\
 & & & & & & & & & & & & & 0
\end{bmatrix} \tag{25}$$

in which three blocks $A_1$, $A_1$, and $D$ are defined in Eqs. (26), (27), and (28).

$$A_1=\begin{bmatrix}
-\frac{3KP_z}{4}-\frac{T(P_++P_-)}{\sqrt{8}} & \frac{AP_z}{2\sqrt{3}}-\frac{\sqrt{3}GP_+}{\sqrt{8}}-\frac{TP_-}{2\sqrt{6}} & \frac{3KP_z}{\sqrt{8}}+\frac{T(P_++P_-)}{2} \\
\frac{AP_z}{2\sqrt{3}}-\frac{\sqrt{3}GP_-}{\sqrt{8}}-\frac{TP_+}{2\sqrt{6}} & \frac{3KP_z}{4}+\frac{T(P_++P_-)}{\sqrt{8}} & \frac{AP_z}{\sqrt{6}}-\frac{\sqrt{3}GP_-}{2}-\frac{TP_+}{2\sqrt{3}} \\
\frac{3KP_z}{\sqrt{8}}+\frac{T(P_++P_-)}{2} & \frac{AP_z}{\sqrt{6}}-\frac{\sqrt{3}GP_+}{2}-\frac{TP_-}{2\sqrt{3}} & 0
\end{bmatrix}, \tag{26}$$

$$A_2=\begin{bmatrix}
-\frac{3KP_z}{4}-\frac{T(P_++P_-)}{\sqrt{8}} & \frac{\sqrt{3}GP_-}{\sqrt{8}}+\frac{TP_+}{2\sqrt{6}}-\frac{AP_z}{2\sqrt{3}} & \frac{3KP_z}{\sqrt{8}}+\frac{T(P_++P_-)}{2} \\
\frac{\sqrt{3}GP_+}{\sqrt{8}}+\frac{TP_-}{2\sqrt{6}}-\frac{AP_z}{2\sqrt{3}} & \frac{3KP_z}{4}+\frac{T(P_++P_-)}{\sqrt{8}} & \frac{\sqrt{3}GP_+}{2}+\frac{TP_-}{2\sqrt{3}}-\frac{AP_z}{\sqrt{6}} \\
\frac{3KP_z}{\sqrt{8}}+\frac{T(P_++P_-)}{2} & \frac{\sqrt{3}GP_+}{2}+\frac{TP_+}{2\sqrt{3}}-\frac{AP_z}{\sqrt{6}} & 0
\end{bmatrix}, \tag{27}$$

$$D=\begin{bmatrix} 0 & \frac{TP_z}{\sqrt{3}}-\frac{\sqrt{3}KP_+}{\sqrt{8}}+\frac{AP_-}{\sqrt{6}} & \frac{TP_z}{\sqrt{2}}+\frac{AP_+}{2}-\frac{3KP_-}{4} \\ \frac{TP_z}{\sqrt{3}}-\frac{\sqrt{3}KP_+}{\sqrt{8}}+\frac{AP_-}{\sqrt{6}} & 0 & \frac{3KP_+}{4}-\frac{AP_-}{2\sqrt{3}}-\frac{TP_z}{\sqrt{6}} \\ \frac{3KP_-}{4}-\frac{AP_+}{2}-\frac{TP_z}{\sqrt{2}} & \frac{\sqrt{3}KP_+}{4}-\frac{AP_-}{2\sqrt{3}}-\frac{TP_z}{\sqrt{6}} & 0 \end{bmatrix}. \tag{28}$$

Here, $A=iQ\cos\Theta(2\cos^2\Theta-\sin^2\Theta)/\hbar$, $G=iQ\sin\Theta(1+\cos^2\Theta)/\hbar$, $K=iQ\sin\Theta\sin 2\Theta/\hbar$, $T=iQ\sin\Theta(2\cos^2\Theta-\sin^2\Theta)/\hbar$, in which $\Theta$ is the angle between **B** and the crystal direction [001]. The other parameters are defined as follows (cf. Ref. 10):

$$\gamma'=\gamma_3+\tfrac{1}{4}\beta^2(\gamma_2-\gamma_3),$$

$$\gamma''=\tfrac{1}{3}(\gamma_2+2\gamma_3)+\tfrac{1}{24}\beta^2(\gamma_2-\gamma_3),$$

$$\gamma'''=\tfrac{1}{3}(2\gamma_2+\gamma_3)-\tfrac{1}{6}\beta^2(\gamma_2-\gamma_3),$$

and

$$\mu_1=-3m\beta\left[\frac{\mu s^2}{2}(aa+a^+a^+)-sc(a^++a)\sqrt{2\mu E_z}\right],$$

$$\mu_2=\sqrt{3}m\left\{\frac{\mu\beta}{2}[s^2(a^+a+aa^+)+aa(3-c^2)]+\sqrt{2\mu E_z}sc[a(5-3c^2)-a^+\beta]-E_zs^2\beta\right\},$$

$$\mu_3=-\sqrt{3}m\{\mu sc[\beta(a^+a+aa^++a^+a^+)-(5-3c^2)aa]+2\beta s[\sqrt{2\mu E_z}sa-E_zc]\},$$

where $\beta=3c^2-1$, $c=\cos\Theta$, $s=\sin\Theta$, and $m=(\gamma_3-\gamma_2)/2$. The definitions of small parameters $q_1,\ldots q_6$ and $c_1,\ldots c_7$ can be found in Ref. 10. (They have the same form in 3LM and 5LM formalisms, since they result from the interactions with distant bands.) Matrix $H^a_{l'l}$ can be solved in terms of a single column of the harmonic-oscillator functions. For $k_z=0$, this matrix factorizes into two $7\times7$ matrices (cf. I).

The part of the eigenvalue problem given by $H^b_{l'l}$ [cf. Eq. (25)] may not be solved by a single column of the harmonic-oscillator functions. Since the bands in GaAs and InP are not strongly nonspherical in the vicinity of the $\Gamma$ point, one can look for solutions of the complete eigenvalue problem (21) in the form proposed by Evtuhov.[30] According to this scheme, each envelope function of the set (20) is developed into a series,

$$f_l(\mathbf{r})=\exp(ik_zz)\sum_m c^l_m|m\rangle,$$

where $|m\rangle$ are the harmonic-oscillator functions and $c^l_m$ are numerical coefficients. This may be regarded as the standard way of transforming an operator eigenvalue problem into an equivalent set of algebraic equations. The algorithm of finding the eigenvalues has been described in I (we usually set $k_z=0$). As compared to the bare 5LM (in which the nonspherical terms are related only to $Q$), there appear now additional matrix blocks related to $\gamma_i$, $q_i$, and $c_i$. In the actual calculations, we used truncated matrices $35\times35$ for $\mathbf{B}\|[001]$, matrices $63\times63$ for $\mathbf{B}\|[110]$, and matrices $42\times42$ for $\mathbf{B}\|[111]$.

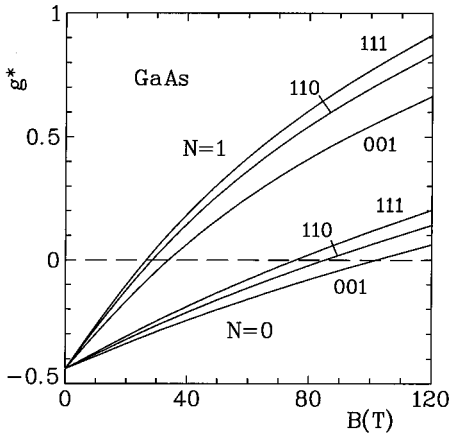


FIG. 8. The Landé factor of conduction electrons in GaAs for the two lowest Landau levels versus magnetic-field intensity, calculated for three field orientations.

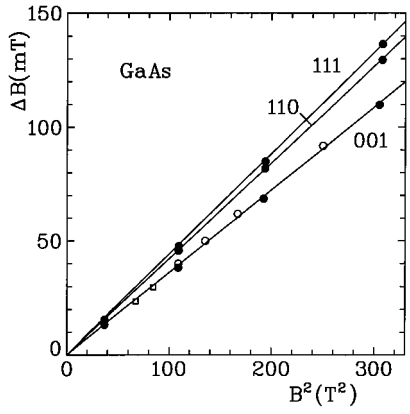


FIG. 9. Spin-doublet splitting of the cyclotron resonance for the conduction electrons in GaAs versus $B^2$ for three field directions. The solid lines are theoretical. Experimental data: open circles, Hopkins *et al.* (Ref. 16); solid circles, Sigg *et al.* (Ref. 34).

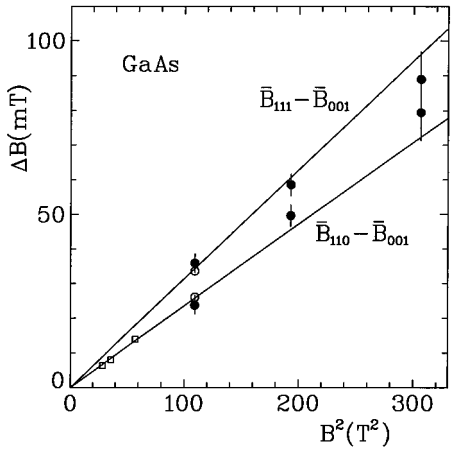


FIG. 10. Shifts of mean cyclotron-resonance field for the conduction electrons in GaAs versus $B^2$ for different field orientations. The solid lines are calculated. Experimental data: open squares, Golubev *et al.* (Ref. 8); open circles, Hopkins *et al.* (Ref. 16); full circles, Sigg *et al.* (Ref. 34).

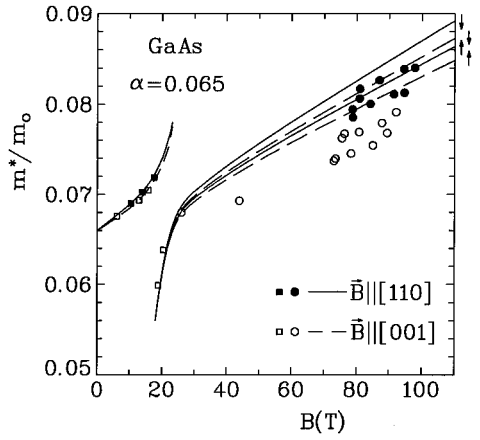


FIG. 11. Cyclotron mass of conduction electrons in GaAs spin-up and spin-down transitions versus magnetic field (megagauss range) for two field orientations. The lines are calculated for the polar constant $\alpha=0.065$ and corresponding adjusted band parameters. Experimental data: squares, Sigg and co-workers (Refs. 34 and 36); circles, Najda *et al.* (Ref. 35).

## VI. RESONANT POLARON EFFECTS

As mentioned in Sec. III, the nonresonant polaron effect is of importance in the determination of the bare electron mass. It has been recognized that in medium gap polar materials GaAs and InP, the resonant polaron effects in the presence of a magnetic field are comparable to the band-structure effects. Thus, the resonant polarons must be included in any precise description of magneto-optical phenomena. Since we have given an explicit description of the electron-phonon interaction and its effects elsewhere,[19] we limit ourselves here to qualitative remarks.

As the energy separation between two Landau levels becomes comparable to the optic-phonon energy $\hbar\omega_l$, the electron in the upper state can make a transition to the lower state with a simultaneous emission of an optic phonon. For $\hbar\omega_c<\hbar\omega_l$, such a transition is virtual. Nevertheless, it influences the energy of the upper Landau state. For $\hbar\omega_c\geq\hbar\omega_l$, the transition is real and the upper state is unstable, i.e., its energy broadens.[31] In the vicinity of the resonance $\hbar\omega_c\approx\hbar\omega_l$ one observes two polaron branches.

In the range of fields $B<20$ T (i.e., below the resonance), the Green-function formalism for the resonant polarons is equivalent to the improved Wigner-Brillouin perturbation theory. Even for the fields $B>80$ T (i.e., high above the resonance), the polaron effects are not negligible and we use the Green-function formalism in their description, including both nonresonant and resonant contributions (cf. Ref. 19).

## VII. P·p THEORY. RESULTS

We now apply the **P**·**p** theory, supplemented by the nonresonant and resonant polaron effects, to the description of various magneto-optical properties of conduction electrons in GaAs and InP. It is the theoretical fit to these data that mainly determines the above quoted values of the adjustable parameters.

The cyclotron-resonance (CR) effective mass $m^*$ is defined by the formula $E(N+1,\pm)-E(N,\pm)=\hbar eB/m^*$. Such a mass depends, in general, on the spin orientation, the intensity and direction of magnetic field, as well as on $N$. The spin $g$ value is defined by the relation $E(N,+)-E(N,-)=g^*\mu_B B$.

### A. GaAs

In Fig. 8, we plot calculated $g^*$ factors for $N=0$ and 1, as functions of the magnetic-field intensity for the principal field directions. It can be seen that the $g$ values change the sign from negative to positive, as functions of energy (or field intensity). This illustrates the common tendency of $g^*$ factors in III-V compounds to reach the free-electron value of $+2$ at high electron energies.[32]

Figure 3 shows the experimental Larmor frequency, measured by Hannak *et al.*,[33] with the use of the quantum beats, compared to our theoretical values $\nu_L=(1/2\pi\hbar)g^*\mu_B B$. The sublinear dependence of $\nu_L$ on $B$ directly indicates that the $g$ value decreases with increasing magnetic field.

Different $g^*$ factors for $N=0$ and 1 Landau levels result in different energies of the cyclotron resonance for spin-up

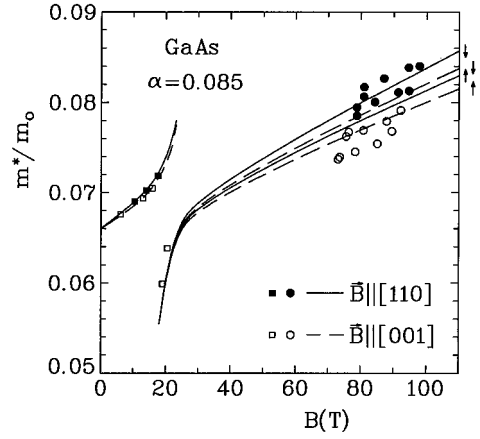


FIG. 12. The same as in Fig. 11, but with the lines calculated for $\alpha=0.085$ and the corresponding adjusted band parameters.

and spin-down transitions. In experiments with a fixed light frequency and swept magnetic field, one observes a spin doublet of CR, in which the higher-energy transition occurs at a lower field. The spin doublets are relatively easy to observe in GaAs since, due to small electron $g$ values, both ground spin states are populated at low temperatures. The spin doublets have been used to demonstrate the necessity of the five-level **P·p** model for GaAs[3] and the nonsphericity of the conduction band in this material.[8] In Fig. 9, we show experimental results on the spin-doublet splitting of CR for the three principal field directions (cf. Refs. 16 and 34), compared to our theoretical description. The splittings $\Delta B$ between two CR peaks are plotted as functions of the average resonance field intensity (squared). The theoretical fit to the anisotropy of the splittings is our main test in determining the parameter $Q$ and the difference $\gamma_3-\gamma_2$ (parameter $Q$ is also important for the determination of the band spin splitting at $B=0$, cf. Sec. IV). As argued in Ref. 3, the spin-doublet splitting is not very sensitive to the polaron effects (which, however, have been included in our description).

In Fig. 10, we show differences of average CR fields measured for different **B** directions: $B_{[111]}-B_{[001]}$ and $B_{[110]}-B_{[001]}$, as functions of magnetic-field intensity (squared). These shifts are directly related to the anisotropy of the electron mass. In contrast to the inadequate description of the mass anisotropy by the simple five-level model (cf. Fig. 11 of I), the inclusion of the far-level contributions in the **P·p** theory allows us to account well for this feature (cf. also Ref. 7). The experimental data do not have the precision of those presented in Fig. 9, since they have been obtained using two separate sweeps of magnetic field, between which the sample had to be rotated.

In Fig. 2, we show the CR masses for the spin-down and spin-up transitions versus the resonant energy, as measured and calculated for **B**$\|$[001]. The increase of the mass is a combined effect of the band's nonparabolicity and the resonant polar interaction (cf. the analysis in I). It should be emphasized that almost identical theoretical descriptions are obtained for the two values of the polar constant $\alpha$, when far-band contributions are properly readjusted (cf. Table I).

Finally, we compare the theory to experiment at megagauss magnetic fields, as performed by Najda *et al.*[35] A plot of CR masses for the two spin orientations versus magnetic field is shown in Fig. 11. The discontinuity of the mass at $B\approx 20$ T is due to the resonant LO-phonon coupling. Using the polar constant $\alpha=0.065$, the theory gives, at megagauss fields, higher masses than those observed experimentally. At high fields, for which $\hbar\omega_c \gg \hbar\omega_L$, the polaron effects are not very important and one deals with almost "bare" electron mass. If one uses a higher value $\alpha=0.085$, the bare mass is lower [cf. Eq. (10)] and the agreement with the experiment is better, as illustrated in Fig. 12. The value of $\alpha=0.085$ gave also a better description of CR emission data, as discussed by Lindemann *et al.*[18] The experimental mass anisotropy at megagauss fields shown in Figs. 11 and 12 is somewhat higher than that predicted theoretically. On the other hand, the situation is reversed at lower fields (cf. Fig. 10).

Figure 13 plots the CR spin-doublet splitting for two field directions up to $B\approx 100$ T. The theory gives a very good description of the experiments at all magnetic fields. However, the experimental resolution at pulsed fields is insufficient to detect a systematic anisotropy of $\Delta B$ for different **B** directions, observed so well at lower dc fields (see Fig. 9).

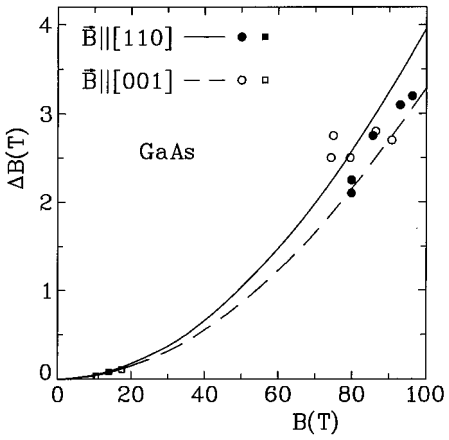


FIG. 13. Spin-doublet splittings of the cyclotron resonance in GaAs versus magnetic field (megagauss range) for two spin orientations. The lines are calculated. Experimental points at ≈80 T are those of Najda *et al.* (Ref. 35).

### B. InP

Figure 14 shows theoretical $g^*$ factors for $N=0$ and 1 Landau levels as functions of magnetic-field intensity for two field directions. In contrast to GaAs, the band-edge $g$ value in InP is positive and, as a result, its energy (or field) dependence is weaker (since it tends to the value of $+2$, see above). Also the difference of $g$ values for the two levels is much smaller in InP than in GaAs. Nevertheless, one can observe the CR spin doublet in this material.

In Fig. 15, we plot the experimental spin-doublet splitting measured by Hopkins *et al.*[16] and our theoretical results. As in the case of GaAs, there is $\Delta B \sim B^2$, but the actual values of $\Delta B$ in InP are considerably smaller than in GaAs, due to the above-mentioned weaker dependence of $g^*$ on $N$.

Figure 6 shows the experimental and theoretical CR masses for two spin orientations, as functions of the reso-

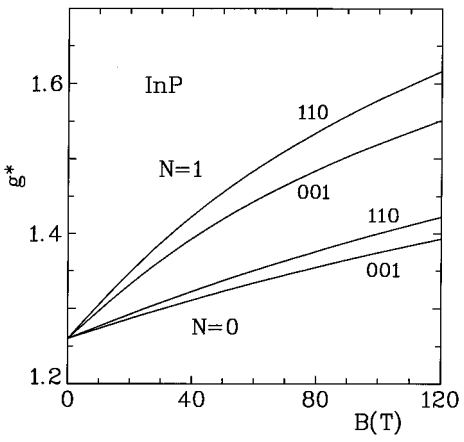


FIG. 14. The Landé factor of conduction electrons in InP for the two lowest Landau levels versus magnetic field intensity, calculated for two field orientations.

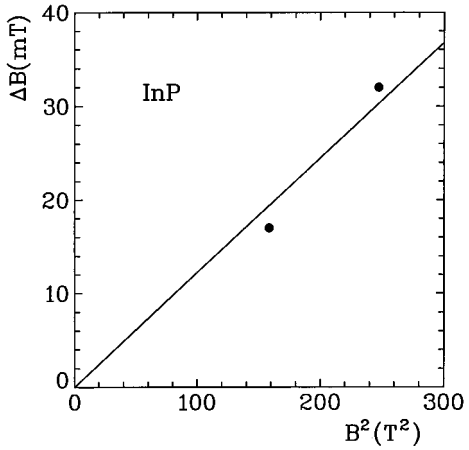


FIG. 15. Spin-doublet splitting of the cyclotron resonance for the conduction electrons in InP versus $B^2$ for $\mathbf{B}\|[001]$. The solid line is theoretical. Experimental data: Hopkins *et al.* (Ref. 16).

nance energy for $\mathbf{B}\|[001]$. As in the case of GaAs, the increase of the mass is due to the combined effect of the band's nonparabolicity and resonant polar interaction. We obtain almost identical theoretical results for $\alpha=0.12$ and 0.20, adjusting properly the far-level parameters (cf. Table IV).

In Figs. 16 and 17, we show the experimental[37] and theoretical CR masses in the megagauss range of fields. The generally accepted for InP polar constant value $\alpha=0.12$ results in too high theoretical masses at high fields. One gets a good description taking $\alpha=0.20$ (cf. Discussion). The megagauss results are, to our knowledge, the only data on the conduction-band nonsphericity in InP. They confirm our value of the parameter $Q$ for this material, determined mainly from the fit to the spin splitting at $B=0$ [cf. Eq. (14) and the Sec. IV].

## VIII. DISCUSSION

As follows from the previous sections the five-level description, supplemented by the main contributions from far

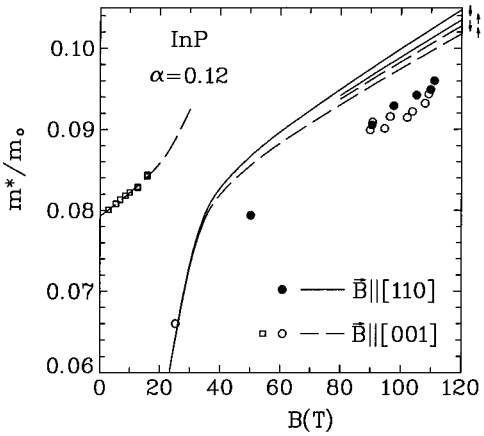


FIG. 16. Cyclotron mass of conduction electrons in InP for spin-up and spin-down transitions versus magnetic field (megagauss range) for two field orientations. The lines are calculated for the polar constant $\alpha=0.12$ and corresponding adjusted band parameters. The experimental data: circles, Najda *et al.* (Ref. 37); squares, Hopkins *et al.* (Ref. 16).

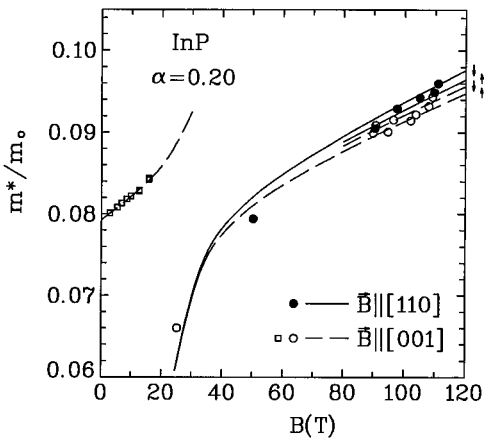


FIG. 17. The same as in Fig. 16, but with the lines calculated for $\alpha=0.20$ and the corresponding adjusted band parameters.

levels, correctly describes various magneto-optical properties of conduction electrons in GaAs and InP. In particular, the far-level contributions allow us to account correctly for the anisotropy of the conduction band in GaAs (cf. Fig. 10), which was not possible with the use of the bare 5LM.

The nonparabolicity of the conduction band in GaAs is of importance for the properties of two-dimensional electron gas in GaAs-$Ga_xAl_{1-x}As$ heterostructures. It was shown by Zawadzki *et al.*[38] (cf. also Ref. 39) that one can carry a rigorous electric and magnetic quantization in such systems using the effective two-level model for nonparabolic bands, as described by Eq. (13). A comparison of various two-dimensional CR data with this model (in particular, those of Hopkins *et al.*, Ref. 40 and Warburton *et al.*, Ref. 41) indicates that our effective gap value $E_0^*=0.98$ eV for GaAs is correct.

The present description accounts also for the megagauss CR data obtained on GaAs and InP, although it requires somewhat higher values of the polar constant $\alpha$ than those usually accepted (cf. Figs. 12 and 17). The required value of $\alpha=0.085$ is quite reasonable for GaAs, it was also required for the CR emission data in this material.[18] For InP, we need $\alpha=0.20$, which was also required for the CR emission data (cf. discussion in Helm *et al.*, Ref. 28). Still, the value of $\alpha=0.20$ for InP seems a little too high. The polar constant is determined by the difference of inverse dielectric constants (for low and high frequencies), so that an even small uncertainty in the determination of one of them may substantially change the value of $\alpha$. It should be mentioned that an equally good description has been obtained for very recent CR data taken on GaAs at magnetic fields of about 200 T,[42] at which the upper $N=1$ Landau level is at the energy $E\approx350$ meV above the conduction-band edge. This testifies to the validity of our model at high electron energies.

As mentioned in the Introduction, one of our main purposes was to develop a theory, which could also describe the valence bands of GaAs and InP. In our multiband scheme, the parameters adjusted to fit the properties of conduction electrons automatically fix the parameters for the valence bands. In Table II, we quote the values of the valence Luttinger parameters $\gamma_1^L$, $\gamma_2^L$, $\gamma_3^L$, $\kappa^L$ for GaAs, as calculated or measured by various authors, together with our values ad-

justed for the polar constants $\alpha=0.065$ and $\alpha=0.085$. [The Luttinger parameters have been calculated using Eqs. (9) from those employed above in 5LM description.] It can be seen that our parameters adjusted for $\alpha=0.085$ are in quite a good agreement with those proposed directly for the valence bands by other authors. Our value of $\gamma_1^L$ is slightly higher, the other two are within the range of other propositions. The light-hole and heavy-hole masses for [100] and [111] directions of **k** are given by the well-known relations:

$$\frac{m_{lh}^{100}}{m_0}=\frac{1}{\gamma_1^L+2\gamma_2^L},\quad \frac{m_{\rm hh}^{100}}{m_0}=\frac{1}{\gamma_1^L-2\gamma_2^L},$$

$$\frac{m_{lh}^{111}}{m_0}=\frac{1}{\gamma_1^L+2\gamma_3^L},\quad \frac{m_{\rm hh}^{111}}{m_0}=\frac{1}{\gamma_1^L-2\gamma_3^L}.$$

The mass values are also quoted in Table II. Our light-hole masses for $\alpha=0.085$ are at the lower end of the values proposed by other authors. The pronounced nonsphericity of the heavy-hole masses and their absolute values are described very well. It can be seen that the $\gamma_1^L$ values adjusted for the polar constant $\alpha=0.065$ differ more from the results of other authors. Thus, the band parameters adjusted for $\alpha=0.085$ are distinctly better for both the high-field conduction-band data (cf. Figs. 11 and 12), as well as for the valence-band data in GaAs. However, one should bear in mind that the experiments concerned with the valence band in this material are still not very precise. For example, the CR results have been obtained at liquid-nitrogen temperatures.[43] This corresponds to the ''semiclassical'' regime in which unequal spacing between the valence Landau levels (due to the $\Gamma_8^v$ degeneracy of the bands) is not observed. Also, at such temperatures, one deals with a modified energy gap and with nonparabolic effects related to the nonnegligible thermal energies of the light holes.

We derive a formula for the mass of the split-off valence band $\Gamma_7^v$, using second-order perturbation theory. The result is (the terms $\Delta^2$ have been neglected)

$$\frac{m_0}{m_{\rm so}}=\gamma_1-\frac{E_{P_0}}{3G_0}+\frac{4\overline{\Delta}\sqrt{E_{P_0}E_{P_1}}}{9(E_1-G_0)G_0}-\frac{2E_Q}{3(G_0-G_1)}. \quad (29)$$

In Table III, we quote hole masses in the split-off valence band of GaAs, as calculated or measured by various authors. Again, our description for $\alpha=0.085$ agrees well with other results.

Tables V and VI quote the hole masses for InP, calculated from our band parameters, as well as those determined directly for the valence bands by other authors. It can be seen that our masses for $\alpha=0.20$ compare quite well with the other results.

Taking into account that, in contrast to the values determined by other authors, we adjust the parameters to obtain a good description of the conduction bands in GaAs and InP and only then use these parameters to describe the valence bands, our hole masses should be considered as very satisfactory.

## IX. CONCLUSION

We have used the five-level **k·p** model supplemented by far-level contributions and polaron effects to describe various magneto-optical data for the conduction bands of medium-gap semiconductors GaAs and InP. A very good description has been obtained for both materials all the way to the megagauss range of magnetic fields. There remains a certain ambiguity between the band-structure effects (resulting from the far-level contributions) and the polaron effects. The band parameters adjusted to fit the conduction-band data give also good values of the hole masses. We conclude that the proposed band model is adequate for both conduction and valence bands of GaAs and InP near the $\Gamma$ point of the Brillouin zone.


[1] E. O. Kane, J. Phys. Chem. Solids **1**, 249 (1957).
[2] C. R. Pidgeon and R. N. Brown, Phys. Rev. **146**, 575 (1966).
[3] W. Zawadzki, P. Pfeffer, and H. Sigg, Solid State Commun. **53**, 777 (1985).
[4] N. R. Ogg, Proc. Phys. Soc. **89**, 431 (1966).
[5] J. M. Luttinger and W. Kohn, Phys. Rev. **97**, 869 (1955).
[6] M. Braun and U. Rossler, J. Phys. C **18**, 3365 (1985).
[7] H. Mayer and U. Rossler, Phys. Rev. B **44**, 9048 (1991).
[8] V. G. Golubev, V. I. Ivanov-Omskii, I. G. Minervin, A. V. Osutin, and D. G. Polyakov, Pis'ma Zh. Eksp. Teor. Fiz. **40**, 143 (1984) [JETP Lett. **43**, 896 (1984)].
[9] R. Grisar, H. Wachering, G. Bauer, J. Wlasak, J. Kowalski, and W. Zawadzki, Phys. Rev. B **18**, 4355 (1978).
[10] M. H. Weiler, R. L. Aggarwal, and B. Lax, Phys. Rev. B **17**, 3269 (1978).
[11] A. Mycielski, J. Kossut, M. Dobrowolska, and W. Dobrowolski, J. Phys. C **15**, 3293 (1982).
[12] U. Rossler, Solid State Commun. **49**, 943 (1984).
[13] M. Cardona, N. E. Christensen, and G. Fasol, Phys. Rev. B **38**, 1806 (1988).
[14] G. E. Pikus, Izv. Akad. Nauk SSSR, Seria Fiz. **52**, 493 (1988).
[15] P. Pfeffer and W. Zawadzki, Phys. Rev. B **41**, 1561 (1990).
[16] M. A. Hopkins, R. J. Nicholas, P. Pfeffer, W. Zawadzki, D. Gauthier, J. C. Portal, and M. A. DiForte-Poisson, Semicond. Sci. Technol. **2**, 568 (1987).
[17] C. Hermann and C. Weisbuch, Phys. Rev. B **15**, 823 (1977).
[18] G. Lindemann, R. Lassnig, W. Seidenbusch, and E. Gornik, Phys. Rev. B **28**, 4693 (1983).
[19] P. Pfeffer and W. Zawadzki, Phys. Rev. B **37**, 2695 (1988).
[20] G. L. Bir and G. E. Pikus, *Symmetry and Strain-Induced Effects in Semiconductors* (Wiley, New York, 1974).
[21] E. O. Kane, in *Narrow Gap Semiconductors, Physics and Application*, edited by W. Zawadzki (Springer, Berlin, 1980), p. 13.
[22] F. H. Pollak, C. W. Higginbotham, and M. Cardona, J. Phys. Soc. Jpn. Suppl. **21**, 20 (1966).
[23] P. Lowdin, J. Chem. Phys. **19**, 1396 (1951).
[24] A. M. White, I. Hinchcliffe, P. J. Dean, and P. D. Green, Solid State Commun. **10**, 497 (1972); C. Weisbuch and C. Hermann, Phys. Rev. **15**, 816 (1977).

[25] W. Zawadzki, Adv. Phys. **23**, 435 (1974).
[26] I. Gorczyca, P. Pfeffer, and W. Zawadzki, Semicond. Sci. Technol. **6**, 963 (1991).
[27] E. Kartheuser, *Polarons in Ionic Crystals and Polar Semiconductors*, edited by J. T. Devreese (North-Holland, Amsterdam, 1972).
[28] M. Helm, W. Knap, W. Seidenbusch, R. Lassnig, and E. Gornik, Solid State Commun. **53**, 547 (1985).
[29] A. T. Gorelonok, V. A. Marushchak, and A. N. Titkov, Izv. Akad. Nauk SSSR, Seria Fiz. **50**, 290 (1986).
[30] V. Evtuhov, Phys. Rev. **125**, 1869 (1962).
[31] M. Nakayama, J. Phys. Soc. Jpn. **27**, 636 (1969).
[32] M. Zawadzki, Phys. Lett. **4**, 190 (1963).
[33] R. M. Hannak, M. Oestreich, A. P. Heberle, and W. W. Ruhle, Solid State Commun. **93**, 313 (1995).
[34] H. Sigg, J. A. A. J. Perenboom, P. Pfeffer, and W. Zawadzki, Solid State Commun. **61**, 685 (1987).
[35] S. P. Najda, S. Takeyama, N. Miura, P. Pfeffer, and W. Zawadzki, Phys. Rev. B **40**, 6189 (1989).
[36] H. Sigg, H. J. A. Bluyssen, and P. Wyder, Solid State Commun. **48**, 897 (1983).
[37] S. P. Najda, H. Yokoi, S. Takeyama, N. Miura, and P. Pfeffer, Phys. Rev. B **44**, 1087 (1991).
[38] W. Zawadzki, C. Chaubet, D. Dur, W. Knap, and K. Raymond, Semicond. Sci. Technol. **9**, 320 (1994).
[39] W. Zawadzki, in *Two-Dimensional Systems, Heterostructures and Superlattices*, edited by G. Bauer *et al.*, Series in Solid State Sciences Vol. 53 (Springer, Berlin, 1984), p. 2.
[40] M. A. Hopkins, R. J. Nicholas, M. A. Brummel, J. J. Harris, and C. T. Foxon, Phys. Rev. B **36**, 4789 (1987).
[41] R. J. Warburton, M. Watts, R. J. Nicholas, J. J. Harris, and C. T. Foxon, Semicond. Sci. Technol. **7**, 787 (1992).
[42] N. Miura *et al.* (unpublished).
[43] M. S. Skolnick, A. K. Jain, R. A. Stradling, J. Leotin, J. C. Qusset, and S. Askenazy, J. Phys. C **9**, 2809 (1976).